PRAMANA
— journal of
physics

Vol. 66, No. 3
March 2006
pp. 521–537

Photorefractive dynamic holography using self-pumped phase conjugate beam

ARUN ANAND[1] and C S NARAYANAMURTHY[2]
[1]Institute for Plasma Research, Bhatt, Near Indira Bridge, Gandhi Nagar 382 428, India
[2]Photonics Laboratory, Applied Physics Department, Faculty of Technology and Engineering, MS University of Baroda, Kalabhavan, P.B. No. 51, Vadodara 390 001, India
E-mail: csnaamu@yahoo.co.in

MS received 29 March 2005; revised 22 December 2005; accepted 29 December 2005

Abstract. Dynamic holography in photorefractive materials using self-pumped phase conjugate beam of the object beam itself as the other writing beam is proposed. Our detailed theoretical analysis shows four-fold increase in the diffraction efficiency of dynamic holograms if recorded using this geometry even in photorefractive crystal like BTO (having low optical activity) without applying external field. Detailed theoretical analysis is given.

Keywords. Photorefractive effect; holography; two-wave mixing; bismuth titanium oxide.

PACS Nos 42.65.Hw; 42.40.Lx; 42.40.Eq

1. Introduction

Photorefractive crystals are by far the most efficient nonlinear optical materials for recording real-time holograms, two-wave mixing experiments for image amplifications, phase conjugation, opto-electronic correlators etc. with relatively low-intensity requirements [1–6]. In particular, photorefractive crystals (PRCs) are widely used for real-time holographic recording because of their practically unlimited recyclability and they can be recorded and erased in this media with sufficiently high sensitivity. The different types of photorefractive crystals which are widely used for real-time holography include, the crystals of sillienite family like bismuth germanium oxide ($Bi_{12}GeO_{20}$ or BGO), bismuth silicon oxide ($Bi_{12}SiO_{20}$ or BSO), bismuth titanium oxide ($Bi_{12}TiO_{20}$ or BTO) and polar crystals like barium titanate ($BaTiO_3$), lithium niobate ($LiNbO_3$) etc. This is because these crystals possess high sensitivity for volume holographic grating formation [7] that enables them to record holograms in the visual region of the spectrum with continuous wave lasers like He–Ne, He–Cd, argon ion etc. Also, these crystals are available in large sizes and are of good quality. Many innovative geometries have been proposed by

various authors to record holograms in these crystals with and without externally applied electric field across the crystal in both two- and four-wave mixing geometries [8–10] respectively. But, in all these cases the diffraction efficiency was not comparable with the conventional holography using photographic emulsions and this will be evident when one records dynamic holographic interferograms using photorefractive crystals. Also, to implement photorefractive holographic interferometry in an industrial environment one must need highly efficient holograms in real-time which should be comparable with conventional holographic and digital speckle pattern interferometry (DSPI) techniques. One of the solutions to increase the diffraction efficiency of the photorefractive holograms is the application of electric field and magnetic field across the crystal [11–13]. But it may be cumbersome to implement such techniques in the industrial environment. Later, a new real-time photorefractive holographic technique using two-wave mixing geometry by exploiting the anisotropic self-diffraction geometry was proposed by Kamshilin *et al* [14] using BTO, which was then implemented using BSO with higher diffraction efficiency by Troth and Dainty [15]. These two dynamic holograms had good efficiency without applied electric field and the main advantage was that one can use polarizer and analyzer pair to separate out diffracted beams. In fact, this two-wave mixing and anisotropic diffraction geometry was very suitable to dynamic holographic interferometry. Again in this case also the diffraction efficiency of the holograms are about 30% for BSO and much less for BTO. So it becomes necessary to develop a technique to improve the diffraction efficiency of the holograms without applying external field in these photorefractive materials.

In this paper we propose a new geometry for recording highly efficient holograms in the photorefractive media using the phase conjugate beam of the signal beam itself as the other writing beam. The advantage of this geometry is that it does not require an externally applied field and the phase conjugate of the signal beam itself serves as the reference beam. A detailed theoretical analysis based on the Kukhtarev's band transport theory [16,17] and necessary experimental conditions required are reported.

2. Theoretical analysis

Figure 1 shows the schematic of the proposed experimental geometry used in this theoretical analysis. The unexpanded laser beam is spatially filtered and then it is collimated by a collimating lens. This beam is allowed to fall on the object as shown in figure 1. The object beam is then divided by the first beamsplitter into two. The reflected beam directly falls on the photorefractive crystal and is the signal beam. The other transmitted object beam is allowed to fall on a perfect phase conjugate mirror (PCM) (which could be $BaTiO_3$ (barium titanate) in self-pumping geometry for the perfect PCM), which in turn sends back the phase conjugate of this beam on to a beamsplitter (BS2). This beamsplitter should be adjusted in such a way that it reflects most of the phase conjugate beam onto a mirror M_3 as shown in figure 1. Then with the help of mirrors M_3 and M_4, the phase conjugate beam is made to fall on the photorefractive crystal.

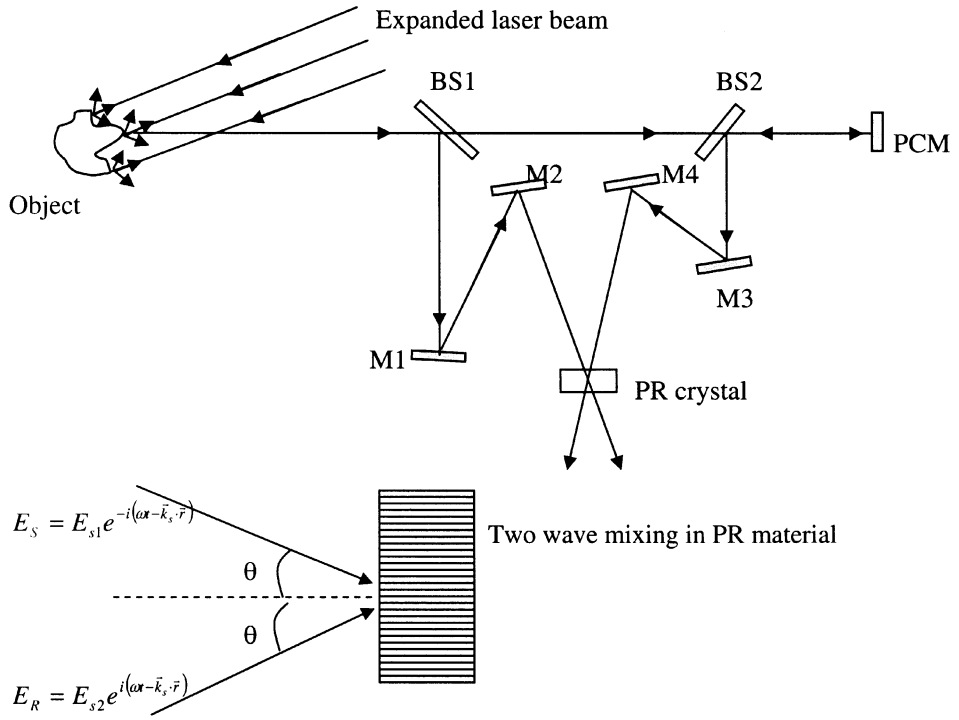

Figure 1. Experimental geometry used in the analysis.

Let $E_{\rm s1}\exp\{-i(\vec{k}\cdot\vec{r}-\omega t)\}$ be the signal beam and $E_{\rm s2}\exp\{-i(\vec{k}\cdot\vec{r}-\omega t)\}$ the conjugate of the signal beam from the phase conjugate mirror falling on the photorefractive crystal. Then the total intensity $I_{\rm t}$ incident on the photorefractive crystal will be

$$I_{\rm t} = I_0\lfloor 1 + M\cos(2\vec{k}_{\rm g}\cdot\vec{x})\rfloor, \tag{1}$$

where $I_0 = I_{\rm s1} + I_{\rm s2}$, with $|E_{\rm s1}|^2 = I_{\rm s1}$, $|E_{\rm s2}|^2 = I_{\rm s2}$, is the average intensity, $M = 2(I_{\rm s1}I_{\rm s2})^{1/2}/I_0$ is the fringe contrast modulation ratio ($0 \le M \le 1$) and $\vec{k}_{\rm g}$ is the fringe pattern wave number. Here we have assumed that the amplitudes of the signal and its phase conjugate are different. Now, if N is the concentration of electrons in the conduction band then the net generation rate of electrons $G_{\rm e}$ will be given by the difference between the rates of generation and recombination of electrons to the donor level, which is equal to

$$G_{\rm e} = (\beta_{\rm e} + sI_{\rm t})(N_{\rm D} - N_{\rm D}^+) - \gamma_{\rm e}NN_{\rm D}^+, \tag{2}$$

where s is the photoionization coefficient, $\gamma_{\rm e}$ is the recombination constant, and $\beta_{\rm e}$ is the thermal excitation rate of electrons. Also $N_{\rm D}$ and $N_{\rm D}^+$ represent the density of the donors and the density of ionized donors respectively and $I_{\rm t}$ is the total light intensity incident on the crystal. Generally, the motion of electrons in the conduction band can be attributed to three forces: (i) drift force due to an external

applied field, (ii) due to photovoltaic effect and (iii) diffusion force due to incident spatially modulated light intensity from regions of higher concentration to regions of lower concentration. So, assuming that the electrons move due to the above forces, the current in the crystal can be written as

$$J_{\mathrm{e}} = eN\mu_{\mathrm{e}}E + \mu_{\mathrm{e}}k_{\mathrm{B}}T\frac{\partial n}{\partial x} + p_n(N_{\mathrm{D}} - N_{\mathrm{D}}^{+})I_{\mathrm{t}}, \tag{3}$$

where μ_{e} is the electron mobility, p_n is the photovoltaic constant, E is the electric field and e is the electric charge. Combining eqs (2) and (3) in continuity equations, we can write the variations of the electron concentration with time as

$$\frac{\partial N}{\partial t} = G_{\mathrm{e}} + \frac{1}{e}\frac{\partial J_{\mathrm{e}}}{\partial x}. \tag{4}$$

In a similar way we can write the continuity equation for density of ionized donors as

$$\frac{\partial N_{\mathrm{D}}^{+}}{\partial t} = G_{\mathrm{e}}. \tag{5}$$

Then, using Poisson's equation the electric field in the crystal can be written as

$$\frac{\partial E}{\partial x} = \frac{e}{\varepsilon_{\mathrm{s}}}(N_{\mathrm{D}}^{+} - N_{\mathrm{A}}^{-} - N), \tag{6}$$

where ε_{s} is the static dielectric permittivity which is independent of position and N_{A}^{-} is the ionized acceptor density. In arriving at eq. (6) we have assumed that the illumination varies only along one dimension. The electrostatic condition implies that

$$\nabla \times \vec{E} = 0. \tag{7}$$

Also assuming that $N \ll N_{\mathrm{A}}$, $N_{\mathrm{D}} - N_{\mathrm{A}}$, $N_{\mathrm{D}}^{+} \approx N_{\mathrm{A}}$, in the steady state, the equation for the number of free electron becomes

$$N = N_0\lfloor 1 + m\cos(2\vec{k}_{\mathrm{g}} \cdot \vec{x})\rfloor, \tag{8}$$

where $N_0 = g(I_0)\tau, g(I_0)$ is the linear generation rate and τ_R is the free electron life-time. Here, m is the reduced fringe contrast modulation ratio given by

$$m = M/(1 + (\beta/sI_0)). \tag{9}$$

Integrating eq. (6) once with respect to x we have the electric field component

$$E = \left(J_{\mathrm{e}} - eD\frac{\partial N}{\partial x}\right) \Big/ e\mu_{\mathrm{e}}N, \tag{10}$$

where D is the diffusion coefficient, $D = \mu_{\mathrm{e}}k_{\mathrm{B}}T/e$. Substituting the respective values for current, number of free electrons etc. and simplifying, eq. (10) reduces to

$$E = \frac{J_{\mathrm{e}}}{e\mu_{\mathrm{e}}N_0} \cdot \frac{1}{1 + m\cos(2k_{\mathrm{g}}x)} - \frac{Dk_{\mathrm{g}}}{\mu_{\mathrm{e}}} \cdot \frac{2m\sin(2k_{\mathrm{g}}x)}{1 + m\cos(2k_{\mathrm{g}}x)}. \tag{11}$$

If the applied voltage is V over a material of length L, then eq. (11) changes to

$$\frac{1}{L}\int_0^L E\,\mathrm{d}x = \frac{V}{L} = \frac{J_\mathrm{e}}{e\mu_\mathrm{e}N_0}\frac{1}{L}\int_0^L \frac{1}{1+m\cos(2k_\mathrm{g}x)}\mathrm{d}x - \frac{Dk_\mathrm{g}}{\mu_\mathrm{e}}\frac{1}{L}\int_0^L \frac{2m\sin(k_\mathrm{g}\cdot x)}{1+m\cos(2k_\mathrm{g}x)}\mathrm{d}x. \tag{12}$$

For integral number of very large numbers of fringes in L,

$$\frac{1}{L}\int_0^L \frac{1}{1+m\cos(2k_\mathrm{g}x)}\mathrm{d}x = \frac{1}{2\sqrt{1-m^2}}\frac{1}{L}\int_0^L \frac{2m\sin(2k_\mathrm{g}x)}{1+m\cos(2k_\mathrm{g}x)}\mathrm{d}x = 0, \tag{13}$$

which implies

$$\begin{aligned} J_\mathrm{e} &= 2(1-m^2)^{1/2}\sigma_0 E_\mathrm{A}, \\ \sigma_0 &= e\mu_\mathrm{e}N_0, \end{aligned} \tag{14}$$

where $E_\mathrm{A} = V/L$ is the applied electric field.

It may be noted that for the applied electric field, the conductivity of cosinusoidal illumination is reduced by a factor $2\sqrt{1-m^2}$ (which is twice less than the conventional photorefractive holography) related to the conductivity at the same average intensity [18]. Rewriting eq. (11) and after simplification we get

$$E = E_\mathrm{A}\cdot\frac{2\sqrt{1-m^2}}{1+m\cos(2k_\mathrm{g}x)} - E_\mathrm{D}\cdot\frac{2m\sin(2k_\mathrm{g}x)}{1+m\cos(2k_\mathrm{g}x)}. \tag{15}$$

In eq. (15), E_D is called as the characteristic field,

$$E_\mathrm{D} = \frac{Dk_\mathrm{g}}{\mu_e} = \left(\frac{k_\mathrm{B}T}{e}\right)k_\mathrm{g}, \tag{16}$$

where T is the room temperature and k_B is the Boltzmann constant. The characteristic field is independent of the material and it depends only on the temperature. If an external electric field is not applied, then charge migration is due to diffusion alone and eq. (15) reduces to

$$E = -E_\mathrm{D}\frac{2m\sin(2k_\mathrm{g}x)}{1+m\cos(2k_\mathrm{g}x)}. \tag{17}$$

Equation (15) is the space-charge field (for diffusion alone) and is denoted by E_sc. In photorefractive materials this space-charge field plays an important role and is created by two different mechanisms using drift (with the applied field) and diffusion (without applied field). The space-charge field which is created due to charge separation will introduce a change in the index of refraction via the linear electro-optic effect (Pockle's effect) and is given by [19,20]

$$\Delta n = \frac{1}{2}n_\mathrm{r}^3 r_\mathrm{eff}E_\mathrm{sc}, \tag{18}$$

where Δn is the change in refractive index, r_{eff} is the effective electro-optic coefficient and n_{r} is the unperturbed refractive index. This change in the index of refraction will lead to a refractive index grating and the diffraction efficiency (η) of such grating is given by [21]

$$\eta = \exp - \left(\frac{\alpha t}{\cos \theta_{\text{B}}} \right) \sin^2 \left(\frac{\pi t}{\lambda \cos \theta_{\text{B}}} \Delta n \right), \tag{19}$$

where α is the absorption coefficient of the crystal, t is the thickness of the crystal, λ is the wavelength of the incident light and θ_{B} is the Bragg's angle inside the crystal. Since, in photorefractive holography both writing and reading holograms are done simultaneously in real-time, the light will diffract from this refractive index grating after mixing. Therefore, there can be transfer of energy from reference (probe) beam to the signal beam. The efficiency of dynamic holograms recorded in the PR crystals depends upon this energy transfer and is known as the photorefractive gain Γ which can be written as [16]

$$\Gamma = \frac{2\pi}{\lambda} n_{\text{r}}^3 r_{\text{eff}} E_{\text{sc}}, \tag{20}$$

where λ is the wavelength of light used. In the following analysis, we will consider in detail the effect of using phase conjugate of the signal beam as the other writing beam in our proposed geometry, on space-charge field (E_{sc}), refractive index change (Δn), diffraction efficiency (η) and gain (Γ) for recording photorefractive hologram in the diffusion regime.

3. Comparative analysis

3.1 *Space-charge field* (E_{sc})

In the absence of an applied electric field, the diffusion phenomenon alone is responsible for the transportation of the photoelectrons in the crystal. This diffusion in the crystal is a result of gradient of the electron density. So, the electrons are generated in the crystal by the illumination of light resulting in a current via diffusion. Due to this the charges are separated. The static electric field thus produced by the build-up of the space charges will move these electrons in the opposite direction. Equation (17) gives a relation between the amplitude of space-charge field (E_{sc}), the diffusion field (E_{D}), the modulation ratio (m) and the grating frequency term (k_{g}). It is sinusoidal and depends on the fringe contrast ratio m, which in turn depends on the relative intensities of the interfering beams (signal and reference). If the illumination is not spatially modulated, but uniform, the fringe contrast or modulation ratio m will be zero and there will not be any induced space-charge field as there is no charge separation. Only when the illumination is spatially modulated, charge separation results due to migration of charges from the brighter region to the darker region. This in turn gives rise to an induced space-charge field. The space-charge field thus depends upon the relative intensities of the writing beams (signal and probe) on the crystal. It is clear from this discussion that space-charge

field plays a crucial role in the formation of index grating. Figures 2 and 3 show the change in space-charge field ($E_{\rm sc}/mE_{\rm D}$), with the fringe contrast ratio m for the conventional photorefractive holographic geometry (diffusion alone) and with applied field. Figure 4 shows our proposed method using phase conjugate signal beam as the other writing beam. It can be seen that the space-charge field $E_{\rm sc}$ increases twice when phase conjugate of the signal beam is used as the reference beam. The grating period decreases by half giving double the number of index of refraction grating lines. Comparing figures 2, 3 and 4 one can clearly see the change in phase shift which is very crucial for the energy exchange in two-wave mixing [22]. The diffusion field $E_{\rm D}$ for plotting these graphs was calculated from eq. (16) under the steady state conditions. The other dependence of space-charge field, is with the grating period (Λ). In fact the electric field will be spatially shifted by a factor of 1/4 of a period relative to the interference fringe pattern [22]. To examine the dependence of the grating period (Λ), a graph is plotted (figure 5) with $E_{\rm sc}$ as a function of Λ for the conventional photorefractive recording and our proposed method. The graph shows a two-fold increase in the space-charge field for the same grating period if the phase conjugate signal beam is used as the other writing beam. The next dependence of space-charge field is with the fringe contrast ratio m. The large fringe contrast ratio will result in higher space-charge field particularly in the diffusion-dominated region which has been proved experimentally [18]. But the main problem is to get large m since the thermal excitations in the crystal will keep it always below 1. In addition to that as m approaches unity the dependence of $E_{\rm sc}$ with m becomes nonlinear [18]. So, it becomes essential to improve the space-charge field using low fringe contrast ratio m. Figure 6 shows a graph for $E_{\rm sc}$ versus fringe contrast ratio m for both the conventional method and our method respectively. It can be seen that our proposed method gives double-fold increase in the space-charge field for all fringe contrast ratios. Table 1 shows the detailed calculation of space-charge field ($E_{\rm sc}$) for a fixed grating spacing of 1 μm (Λ) and for various fringe contrast values (m) in the conventional method and our geometries respectively. For this calculation the diffusion field $E_{\rm D}$ is equal to 1.625 kV/cm.

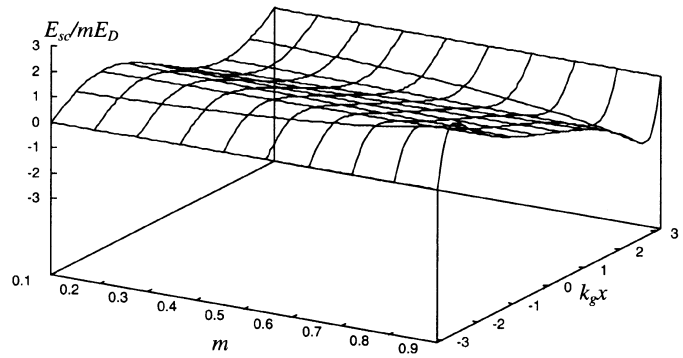

Figure 2. Change in space-charge field as a function of fringe modulation ratio and phase for conventional photorefractive holography.

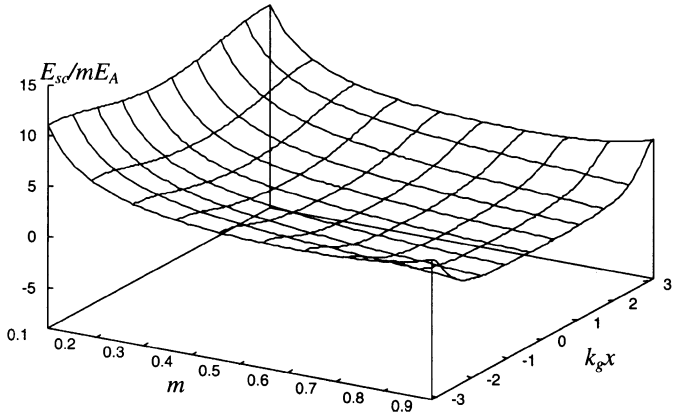

Figure 3. Change in space-charge field as a function of fringe modulation ratio and phase for conventional photorefractive holographic method with an externally applied electric field.

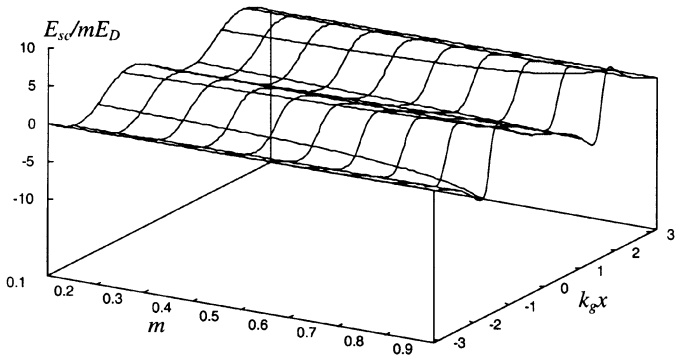

Figure 4. Change in space-charge field as a function of fringe modulation ratio and phase when phase conjugate beam of the signal beam is used as reference beam.

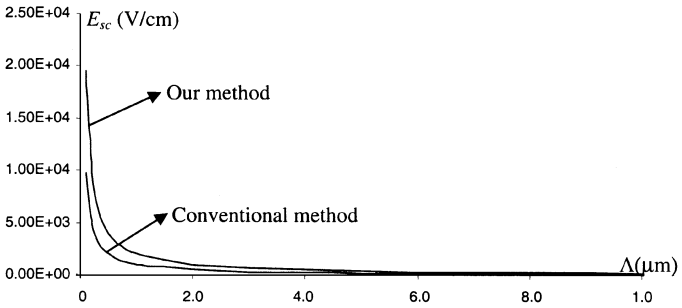

Figure 5. Space-charge field as a function of grating element ($m = 0.6$).

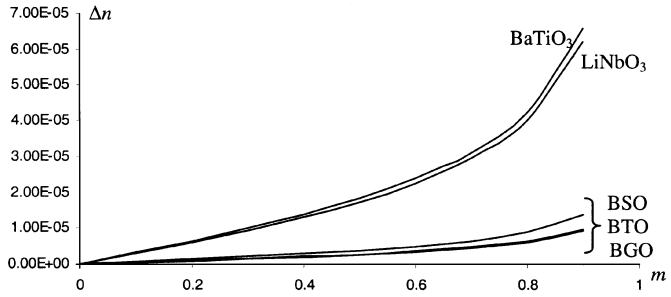

Figure 6. Space-charge field as a function of fringe contrast ratio.

Table 1. Space-charge field for different fringe contrast ratios ($\Lambda = 1$ μm).

Fringe contrast ratio (m)	E_{sc} (V/cm)	
	Conventional method	Our method
0.0	0	0
0.1	0.1634	0.3268
0.2	0.3319	0.6637
0.3	0.5113	1.0222
0.4	0.7095	1.4190
0.5	0.9386	1.8773
0.6	1.2193	2.4382
0.7	1.5935	3.1689
0.8	2.1677	4.3335
0.9	3.3657	6.7135

3.2 *Refractive index change* (Δn)

The next important parameter considered in our analysis is the change in index of refraction (Δn). Equation (18) gives the relationship of Δn with the space-charge field (E_{sc}), unperturbed refractive index (n_r) and the electro-optic coefficient (r_{eff}). Since the refractive index change is directly proportional to the space-charge field, it is straightforward to find the increment if our method is used instead of the conventional two-wave mixing geometry. The physical parameters of PR materials, which were used in our calculation, are listed in table 2. The change in index of refraction was calculated for different m and the results are plotted for the conventional method (figure 7) and our geometry (figure 8). As expected, the polar crystals like barium titanate ($BaTiO_3$) and lithium niobate ($LiNBO_3$) are having maximum change due to their large unperturbed refractive index (n_r) and high electro-optic coefficient (r_{eff}). Among the PR materials of the sillienite family, bismuth silicon oxide (BSO) is having the maximum change in refractive index (table 3). The change in index of refraction for two other crystals of the sillienite family, i.e. BTO and BGO, have similar values. From figures 7 and 8, it is clear that for all these crystals the value of Δn doubles if the phase conjugate signal beam is used as the other writing beam.

Table 2. Physical properties of photorefractive materials ($\lambda = 633$ nm, $\Lambda = 1\,\mu$m) [37–39].

Photorefractive crystals	Unperturbed refractive index n_r	Linear electro-optic coefficient r_{ij} (cm V^{-1}) $\times 10^{-10}$	Absorption coefficient α (cm^{-1})
$Bi_{12}SiO_{20}$	2.54	5.00 (r_{41})	1.3
$Bi_{12}GeO_{20}$	2.54	3.40 (r_{41})	1.3
$Bi_{12}TiO_{20}$	2.25	5.17 (r_{41})	0.3
$LiNbO_3$	2.29	30.8 (r_{33})	0.3
$BaTiO_3$	2.41	28.0 (r_{33})	0.3

Table 3. Calculated index of refraction change and diffraction efficiency ($\Lambda = 1$ μm, $\lambda = 632.8$ nm, $t = 10$ mm, $\theta_B = 18.445°$).

		Conventional method		Our method	
PR material	Fringe contrast ratio (m)	$\Delta n \times 10^{-6}$	η (%)	$\Delta n \times 10^{-6}$	η (%)
	0.1	3.202	2.021	6.403	7.861
$BaTiO_3$	0.3	10.019	18.218	20.032	54.648
	0.4	13.904	32.167	27.808	71.917
	0.1	3.021	1.802	6.043	7.030
$LiNbO_3$	0.3	9.455	16.391	18.904	50.809
	0.4	13.122	29.225	26.244	70.055
	0.1	0.669	0.031	1.338	0.124
$Bi_{12}SiO_{20}$	0.5	3.845	1.013	7.690	3.893
	0.9	13.752	11.030	27.503	25.009
	0.1	0.481	0.046	0.962	0.184
$Bi_{12}TiO_{20}$	0.5	2.763	1.509	5.527	5.913
	0.9	9.883	17.774	19.768	53.770
	0.1	0.455	0.014	0.910	0.057
$Bi_{12}GeO_{20}$	0.5	2.614	0.472	5.229	1.853
	0.9	9.351	5.608	18.702	17.492

3.3 *Diffraction efficiency* (η)

Unlike Bragg diffraction from index gratings, the diffraction of light from the volume holographic gratings formed inside a photorefractive medium is different. The diffractions from volume holographic gratings in the photorefractive medium can be from two-wave mixing as well as from four-wave mixing. In the latter case, a third beam is used to read out the hologram at a Bragg angle. In fact the incident read-out beam and diffracted signal beam can create another new photorefractive grating thus making it more complicated. So, the diffraction efficiency (η) for a

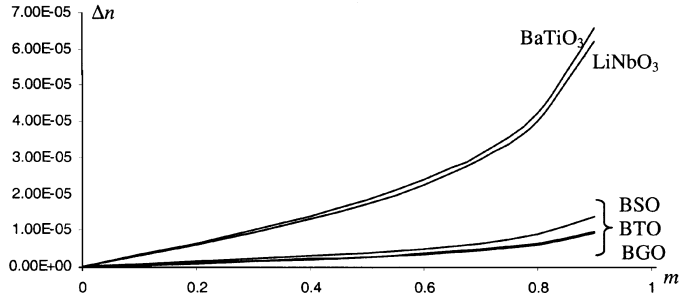

Figure 7. Change in index of refraction as a function of fringe modulation ratio for conventional photorefractive holography.

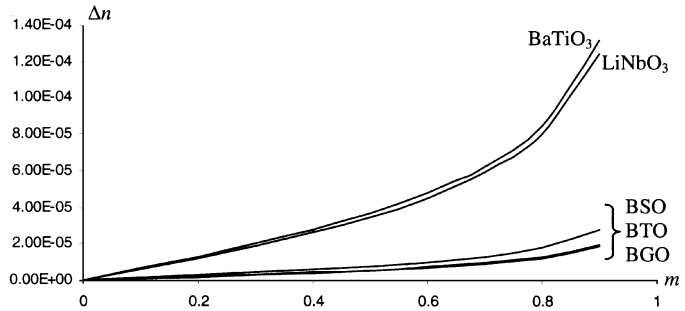

Figure 8. Change in index of refraction as a function of fringe modulation ratio when phase conjugate beam of the signal beam is used as the reference beam.

photorefractive hologram can be defined as the fraction of power of the incident beam (read or probe) which is transferred at a distance t into the diffracted beam from the volume holographic grating formed in a photorefractive medium. It may be noted that the read or probe beam need not have the same wavelength as that of the writing beams. The relation between the diffraction efficiency (η) and other parameters like the absorption coefficient (α), the thickness of the PR crystal (t), the wavelength of light used (λ), the Bragg's angle (θ_{B}) and most importantly the change in the index of refraction (Δn) is given in eq. (19). The calculated diffraction efficiencies ($\eta\%$) for various modulation ratios using the conventional method and our method are tabulated in table 3. The thickness t of the crystal was assumed to be 10 mm for all the considered crystals in the calculations. We have also plotted graphs (figures 9 and 10) showing the variation of diffraction efficiency (η) with fringe contrast ratio m for both the holographic methods respectively. On examining these figures one can see that the diffraction efficiencies increase almost four times when our method is used. As m increases the relationship between m and η becomes highly nonlinear. But, for the region $m < 0.6$ the relationship is almost linear [18]. In this region also the diffraction efficiency increases almost four times for the proposed method. If barium titanate is used as the recording medium then it achieves a diffraction efficiency of $\approx$75% for a modulation depth of 0.4 in the proposed method but, to achieve the same using the

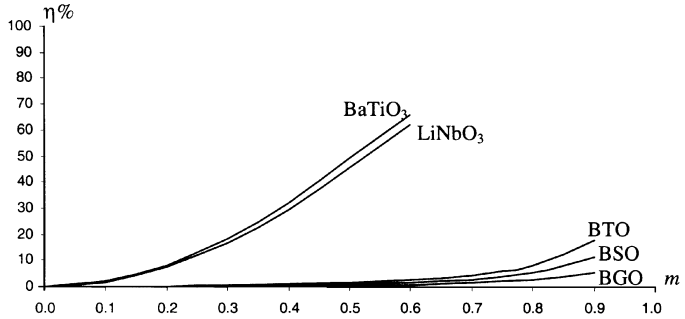

Figure 9. Diffraction efficiency as a function of fringe modulation ratio for conventional photorefractive holography.

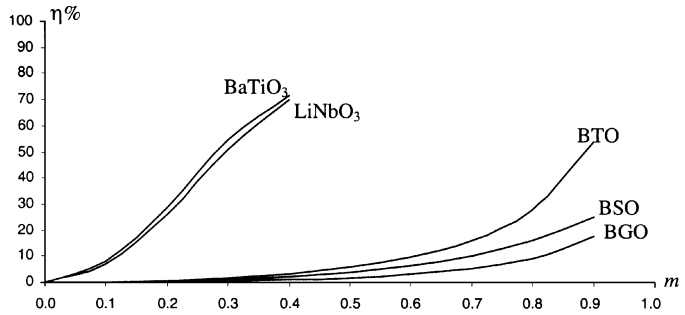

Figure 10. Diffraction efficiency as a function of fringe modulation ratio when phase conjugate beam of the signal beam is used as the reference beam.

conventional method a modulation depth of $m = 0.7$ is required. Among the photorefractive materials of sillienite family, BTO shows maximum diffraction efficiency for a particular m even though its change in index of refraction (Δn) is less than that of BSO. This is because its absorption coefficient ($\alpha = 0.3$/cm) is less than the absorption coefficient of BSO ($\alpha = 1.3$/cm) at a particular wavelength (633 nm). We have compared our results with the established experimental results. Herriau *et al* [23] reported a diffraction efficiency of 95% for BGO under an externally applied DC field (E_{A}) of 14 kV/cm using an incident light of wavelength 514 nm and grating spacing of 20 μm for a crystal of 10 mm thickness. But, our method can give a diffraction efficiency of ≈22% without using any externally applied field for a modulation depth of 0.9 and grating spacing of 1 μm. Kamishilin *et al* [24] obtained a diffraction efficiency of 30% for diffusion recording in BTO. Using our method, a diffraction efficiency of ≈55% can be achieved for a modulation depth of 0.9 for the same diffusion recording. Huignard and Micheron [25] and Peltier and Micheron [26] obtained a diffraction efficiency of 5% for holographic recording with an external DC field (E_{A}) of 10 kV/cm ($t = 10$ mm, $\lambda = 514$ nm) in BSO. We calculated a diffraction efficiency of 6% for BSO with a modulation depth of 0.5 for a crystal of 10 mm thickness using an incident light of $\lambda = 514$ nm and grating

Table 4. Calculated photorefractive gain.

Fringe contrast ratio (m)	Photorefractive gain (Γ) (cm^{-1})									
	Conventional method					Our method				
	$BaTiO_3$	$LiNbO_3$	BSO	BTO	BGO	$BaTiO_3$	$LiNbO_3$	BSO	BTO	BGO
0.0	0	0	0	0	0	0	0	0	0	0
0.1	0.635	0.600	0.132	0.095	0.090	1.271	1.200	0.265	0.191	0.090
0.2	1.291	1.218	0.269	0.194	0.183	2.582	2.437	0.539	0.388	0.183
0.3	1.989	1.877	0.415	0.298	0.282	3.977	3.754	0.831	0.597	0.282
0.4	2.761	2.605	0.577	0.414	0.392	5.522	5.211	1.154	0.829	0.392
0.5	3.652	3.447	0.763	0.548	0.519	7.305	6.894	1.527	1.097	0.519
0.6	4.745	4.478	0.991	0.712	0.674	9.488	8.954	1.983	1.425	0.674
0.7	6.201	5.852	1.296	0.931	0.881	12.402	11.704	2.592	1.863	0.881
0.8	8.435	7.960	1.763	1.267	1.199	16.865	15.916	3.525	2.534	1.199
0.9	13.062	12.327	2.730	1.962	1.856	26.125	24.655	5.461	3.925	1.856

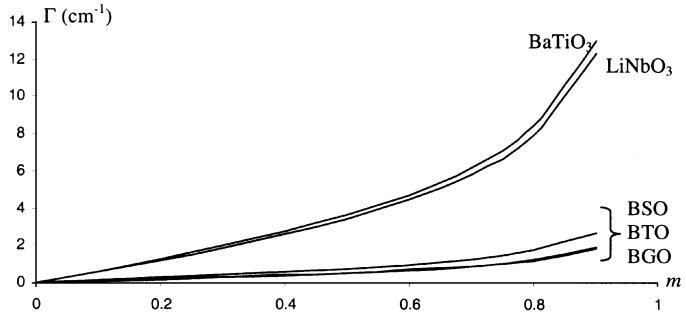

Figure 11. Photorefractive gain as a function of fringe modulation ratio for conventional photorefractive holography.

spacing of 1 μm. Diffraction efficiencies of almost 100% were reported for diffusion recording of holograms in lithium niobate [27–29]. We calculated a diffraction efficiency of 70% for a modulation depth of 0.4 whereas the conventional method yielded a diffraction efficiency of only 29% for the same modulation depth (Λ = 1 μm, $\lambda = 632.8$ nm, $t = 10$ mm). Table 5 gives a comparison between the reported values and the values calculated using our proposed method.

3.3 *Photorefractive gain* (Γ)

Photorefractive gain (Γ) gives the amount of transferred energy from the reference beam to the signal beam while writing a hologram in photorefractive media. Equation (20) relates it with other parameters. The gain is inversely proportional to the wavelength of light used for holographic recording. We have calculated the photorefractive gain for various photorefractive crystals in the diffusion region for both conventional method and our method respectively as shown in table 4. Figures 11 and 12 give the graphs for Γ versus modulation ratio m for both the methods

Table 5. A comparative look.

		PR parameters – reported values					PR parameters obtained using our method				
PR material	λ (nm)	E_A (kV/cm)	Λ (μm)	t (mm)	η (%)	Γ (cm^{-1})	m	Λ (μm)	t (mm)	η (%)	Λ (cm^{-1})
BGO	514.0	14.00	20.00	10.00	95.00 [23]	–	0.9	20.00	10.00	0.10	0.46
							0.9	1.00	10.00	22.20	4.57
	605.0	11.00	10.00	9.15	–	2.30 [39,40]	0.9	10.00	9.15	0.25	0.39
							0.9	1.00	9.15	18.50	3.90
BSO	514.0	10.00	–	10.00	5.00 [22,23]		0.6	1.00	10.00	5.74	1.88
							0.9	1.00	10.00	25.20	6.72
	514.0	19.00	4.00	–	–	1.00 [30]	0.6	4.00	10.00	0.65	0.61
							0.9	4.00	10.00	9.14	2.44
BTO	632.8	15.00	2.50	–	–	10	0.6	2.50	10.00	1.63	0.57
			to			to	0.9	2.50	10.00	11.80	1.57
			10.00			15 [37,38]					
	632.8	0.00	–	–	30.00 [24]	–	0.9	1.00	10.00	53.80	3.93
$LiNbO_3$	632.8	0.00	–	–	≈100 [27–29]	–	0.4	1.00	10.00	70.10	5.21
	632.8	0.00	0.30	–	10.00 [30]	–	0.6	0.30	10.00	72.9	29.80

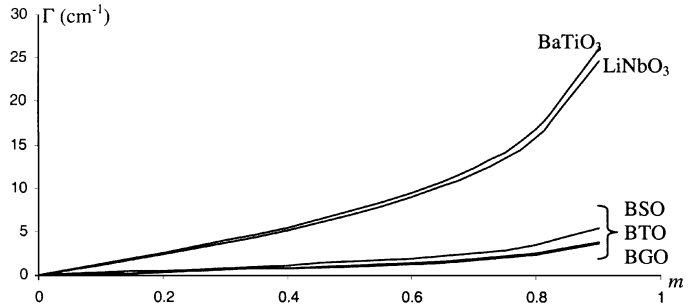

Figure 12. Photorefractive gain as a function of fringe modulation ratio when phase conjugate beam of the signal beam is used as the reference beam.

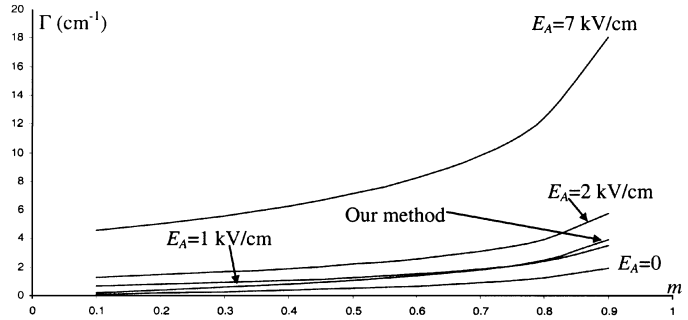

Figure 13. Photorefractive gain as a function of fringe contrast ratio using conventional PR holographic method with an externally applied electric field and using our method.

respectively. The advantage of using our method can be seen from the figures as the photorefractive gain doubles. The maximum gain obtained is when $BaTiO_3$ is used as the recording medium. Its calculated gain was $\approx$26 cm^{-1} for a modulation depth of 0.9, whereas for the conventional method a gain of only $\approx$13 cm^{-1} was obtained for the same modulation depth. Photorefractive gain of 10 cm^{-1} was observed for $LiNbO_3$ via diffusion grating ($\Lambda = 0.3$ mm, $\lambda = 632.8$ nm) [30] and with applied fields of 5–10 kV/cm the gain was reported to be a few tens cm^{-1} [31,32]. We calculated a PR gain of $\approx$13 cm^{-1} using $\Lambda = 0.3$ mm and $\lambda = 632.8$ nm for a modulation depth of 0.2 when phase conjugate beam of the signal beam is used as the reference beam. The calculated gain for $LiNbO_3$ in our case was up to 25 cm^{-1} for a modulation depth of 0.9, which is equivalent to applying an external field of 5–10 kV/cm. A gain of 2.4 cm^{-1} to 12 cm^{-1} was reported using various methods for BSO using an externally applied DC and alternating electric fields of up to 19 kV/cm ($\lambda = 514$ nm) [22,33–36]. We calculated a gain of 7 cm^{-1} in BSO (table 5) for a modulation depth of 0.9 ($\lambda = 514$ nm, $\Lambda = 1$ mm) indicating that our method can be used to increase the gain without applying external electric field. Stepanov *et al* [37,38] reported a gain of 10–15 cm^{-1} with an externally applied electric field of 15 kV/cm in BTO. But, our calculations showed a gain of 4 cm^{-1} for a modulation depth of 0.9 without any applied field if phase conjugate signal beam is used as the

other writing beam. Finally the graph in figure 13 gives the comparison between the gain obtained using the applied electric field and the proposed method. For large fringe contrast ratio (m) our method can give more gain than applying 1 kV electric field across the crystal.

We recommend an argon ion laser with 1 W power at 514 nm as the source, with an undoped $BaTiO_3$ (barium titanate) crystal as the phase-conjugate mirror in its self-pumped phase conjugation geometry and a $Bi_{12}SiO_{20}$ (bismuth silicon oxide) crystal as the holographic recording medium. Another important factor is that this proposed geometry is more suitable for transparent phase object holography, where most of the incident object beam is transmitted.

4. Conclusion

A new geometry using the phase conjugate signal beam as the other writing beam for recording real-time photorefractive holography is proposed. Our detailed calculations show many-fold increase in the diffraction efficiency and photorefractive gain in the diffusion recording without applying external electric field across the crystal. This proposed geometry will be ideal for real-time holographic photo-elasticity to study photo-elastic materials under stress, where objects are transparent. It may be noted here that the suggested necessary power of the laser beam for this proposed geometry is similar to or less than the power required to record dynamic holograms even with applied field in photorefractive BSO.

Acknowledgement

The authors gratefully acknowledge the Department of Science and Technology (DST), Government of India and the University Grants Commission (UGC), New Delhi for providing financial assistance through their respective project grants (SP/S2/L-15/94) and F-10-7/2001(SR-1) to carry out this work. One of the authors (AA) acknowledges the DST for providing the JRF through the same grant. The authors would also like to thank the referee for his comments and suggestions to improve the manuscript.

References

[1] A Yariv, *IEEE J. Quantum Electron.* **14**, 650 (1978)
[2] A Yariv and P Yeh, *Optical waves in crystals* (Wiley, 1984) Chap. 13
[3] F Laeri, T Tschudi and J Albers, *Opt. Commun.* **47**, 387 (1983)
[4] D Plastis, J Yu and J Hong, *Appl. Opt.* **24**, 3860 (1985)
[5] J P Huignard and A Marrakchi, *Opt. Lett.* **6**, 622 (1981)
[6] H Rajenbach, S Bann, P Refregier, P Joffre, J P Huignard, H S Buchkremer, A S Jensen, E Rasmussen, K H Brenner and G Lohmann, *Appl. Opt.* **31**, 5666 (1992)
[7] J P Huignard, J P Herriau and T Valentin, *App. Opt.* **16**, 2796 (1977)
[8] J P Huignard, J P Herriau, P Aubourg and E Spitz, *Opt. Lett.* **4**, 21 (1979)
[9] A Marrakchi, R V Johnson and A R Tranguay Jr, *J. Opt. Soc. Am.* **B3**, 321 (1986)

[10] J M Haeton and L Solimar, *IEEE J. Quantum Electron.* **24**, 558 (1988)
[11] S I Stepanov and M P Petrov, *Opt. Commun.* **53**, 292 (1985)
[12] G Pauliat and G Roosen, *J. Opt. Soc. Am.* **B7**, 2259 (1990)
[13] A Grunnet-Jepsen, I Aubrecht and L Solimar, *J. Opt. Soc. Am.* **B12**, 921 (1995)
[14] A A Kamshilin, E V Mokrushina and M P Petrov, *Opt. Engg.* **28**, 580 (1989)
[15] R C Troth and J C Dainty, *Opt. Lett.* **16**, 53 (1991)
[16] N V Kukhtharev, V B Markov, S G Odulov, M S Soskin and V L Vinetskii, *Ferroelectrics* **22**, 949 (1979)
[17] N V Kukhtharev, V B Markov, S G Odulov, M S Soskin and V L Vinetskii, *Ferroelectrics* **22**, 961 (1971)
[18] T J Hall, R Jaura, L M Connors and P D Foote, *Prog. Quant. Electr.* **10**, 77 (1985)
[19] P Yeh, *Introduction to photorefractive nonlinear optics* (John Wiley & Sons Inc., New York, 1993)
[20] L Solimar, D J Webb and A Grunnet-Jepsen, *The physics and applications of photorefractive materials*, Oxford Series in Optical Imaging and Sciences (Clarendon Press, Oxford, 1996)
[21] H Kogelnik, *Bell Syst. Tech. J.* **48**, 2909 (1969)
[22] S I Stepanov and M P Petrov, Nonstationary holographic recording for efficient amplification and phase conjugation, in: *Photorefractive Materials and Applications I*, *Topics Appl. Phys.* edited by P Gunter and J P Huignard (Springer, Berlin, Heidelberg, 1988) Vol. 61
[23] J P Herriau, D Rojas, J P Huignard, J M Bassat and J C Launay, *Ferroelectrics* **75**, 271 (1987)
[24] A A Kamishilin, S V Miridonov, M G Miteva and E V Mokrushina, *Sov. Phys. Tech. Phys.* **34**, 66 (1989)
[25] J P Huignard and F Micheron, *Appl. Phys. Lett.* **29**, 591 (1976)
[26] M Peltier and F Micheron, *Appl. Phys. Lett.* **48**, 3683 (1977)
[27] J J Amodei and D L Staebler, *RCA Rev.* **33**, 71 (1972)
[28] K G Belabaev, V B Markov and S G Odulov, *Ukr. Fiz. Zh.* **24**, 366 (1979)
[29] V L Vinetskii, N V Kukhtharev, V B Markov, S G Odulov and M S Soskin, *Bull. Acad. Sci. USSR, Phys. Ser.* **41**, 135 (1977)
[30] V L Vinetskii, N V Kukhtharev, V B Markov, S G Odulov and M S Soskin, pre-print No. 15 (Inst. of Phys. of Ukr. Acad of Sci., Kiev, 1976)
[31] N V Kukhtarev, V B Markov and S G Odulov, *Opt. Commun.* **23**, 338 (1977)
[32] V P Kondilenko, V B Markov, S G Odulov and M S Soskin, *Ukr. Fiz. Zh.* **23**, 2039 (1978)
[33] A Marrrakchi, J P Huignard and P Gunter, *Appl. Phys.* **24**, 131 (1981)
[34] H Rajenbach, J P Huignard and B Loiseaux, *Opt. Commun.* **48**, 247 (1983)
[35] J P Huignard and A Marrrakchi, *Opt. Commun.* **38**, 249 (1981)
[36] P Refregier, L Solimar, H Rajenbach and J P Huignard, *Electron. Lett.* **20**, 656 (1984)
[37] G S Trofimov and S I Stepanov, *Sov. Tech. Phys. Lett.* **11**, 256 (1985)
[38] S I Stepanov and M P Petrov, *Opt. Commun.* **53**, 292 (1985)
[39] M P Petrov, S I Stepanov and A V Khonenko, *Photorefractive crystals in coherent optical systems* (Springer-Verlag, Berlin, 1991) Vol. 59, pp. 222–241
[40] P Gunter, *Opt. Commun.* **41**, 83 (1982)